

Pit Growth Behavior on Aluminum under Potentiostatic Control

Lei Yao, Jianhua Liu^{*}, Songmei Li, Mei Yu

School of Materials Science and Engineering, Beihang University, Beijing 100191, China

*E-mail: liujh@buaa.edu.cn

Received: 2 March 2014 / *Accepted:* 29 March 2014 / *Published:* 14 April 2014

The growth behavior of pits on aluminum is studied during potentiostatic etching with current transient measurement, SEM and AFM observation. The results show that there is an induction period for the pit nucleation. The current rises to a maximum and then a plateau appears during the etching. Hemispherical pits form and grow in size before the plateau, and transform into half-cubic pits at the plateau. The change of the pitting behavior is controlled by the current density for pitting.

Keywords: Aluminum; Pitting corrosion; Potentiostatic; Electrochemical etching.

1. INTRODUCTION

Electrochemical etching is a promising method for fabricating microstructures of metal or semiconductor substrates due to its capability for high throughput manufacturing of microstructures [1-7]. Electrochemical etching of Al is generally used in capacitor industry to produce high surface area electrodes for electrolytic capacitors because the pitting corrosion during the etching process greatly improves the specific surface area of Al surface [8-14]. Since the pit nucleation and growth are essential steps in electrochemical etching process, recently interests have been aroused in the effort to control the nucleation and growth of pits more precisely [6-7, 15-18].

The electrochemical etching in common application is performed under the control of current. Imposing a constant anodic current on Al produces an anodic potential transient during the initial interval of hundreds of milliseconds [19-24]. The potential usually rises for a while before steeply dropping to a plateau. The duration of the potential rise is typically 10-100 ms and is dependent up on the specimen's thermal and chemical history [22-26]. The steady-state potential at the plateau is considered as the repassivation potential, at which both passivation and dissolution occur [23]. It has

been reported that hemispherical pits grow during the potential rise interval [19-20]. However, the details of the pit growth behavior under different potentials are yet to be clarified, and only a few studies concern the influence of potential on pit nucleation and growth [20, 25]. This work focuses exclusively on the growth behavior of pits under the potentiostatic control to provide further insight into the electrochemical etching process of Al.

2. EXPERIMENTAL

Specimens were cut from Al foil of 110 μm thickness. This type of foil has a high purity of 99.99% and a proper structure with high cubic texture. A large proportion of the exposed foil surface is (1 0 0) face in crystallography. This type of foil is generally used to produce electrodes in capacitor industry.

Each specimen was pretreated in 1 M NaOH solution at 50 °C for 1 minutes, followed by immersion in 1 M HNO₃ bath at room temperature for 30 seconds. Then the specimen was rinsed thoroughly with deionized water and blown dry with cool air. After the pretreatment, the specimen was mounted in a holder having an exposed area of 1 cm² and transferred into 1 M HCl solution at 30 °C. The following electrochemical experiments were conducted with the three electrode system. A Pt plate worked as the counter electrode and the saturated calomel electrode (SCE) worked as the reference electrode. The specimen was immersed in the electrolyte at open circuit for about 3 minutes, so that its open circle potential (OCP) reached steady state. Then the specimen was electrochemically etched up to several hundreds milliseconds under a static potential condition. A potentiostat/galvanostat (PARSTAT2273, Ametek, US) was used to carry out the etching and record the current transient.

The etched specimens were observed with scanning electron microscope (SEM) (CS3400, Camscan, UK) to examine the morphology of pits on the surface. Pit density was measured as the total pits counted on 10 micrographs at 500 \times magnification, each covering a randomly selected area of 240 \times 192 μm . Pit size distribution was determined from the analysis of 20 micrographs at 1000 \times magnification, each covering 120 \times 96 μm . Three dimensional structures of the pits were examined with atomic force microscope (AFM) (Dimension Icon, Veeco, USA).

3. RESULTS AND DISCUSSION

3.1 Current transient during potentiostatic etching

Fig. 1a shows the current-time curves of a series of potentiostatic etching experiments in which the potential parameter varies from -0.7 V to -0.4 V (vs. SCE). Fig. 1b is a magnification of Fig. 1a during the first 150 ms etching. It shows that an initial jump appears in all curves immediately after the potential of specimen steps to the setting value, and the current value of the jump increases sharply with the etch potential. After the initial jump, the current decreases for dozens of milliseconds followed by a continuous increase. No pitting corrosion is found under the SEM observation until the

current starts to increase. It indicates that there is an initial induction stage for the pitting, and the duration before the current reaches the minimum is the induction period of the pit nucleation. As the etch potential shifts from -0.7 V to -0.4 V, the induction period decreases obviously from about 100 ms to 20 ms. It indicates that the potential parameter has a significant influence on the pit nucleation. It is known that the electrochemical behavior during etching has much relation to thermal and chemical history of specimens [26]. Al surface after the pretreatment in this work is covered with a native oxide film of several nanometers in thickness. As the etch potential becomes more noble, it turns easier for aggressive ions to penetrate into the film and initiate a pit, so that the induction period of the pit nucleation reduces. Moreover, for the etching experiments at the potential above -0.6 V, the current rises for about 5 ms before it drops, resulting in a peak in the current-time curves during the induction period. The shape of the peak turns steeper while the etch potential shifts from -0.55 V to -0.4 V.

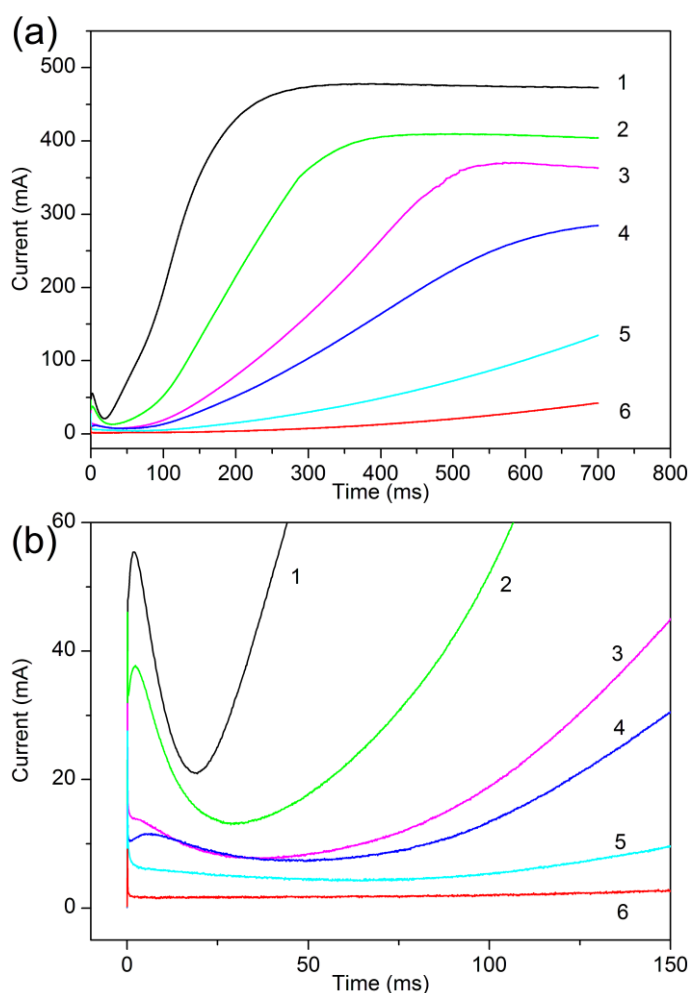


Figure 1. (a) Current-time curves of Al specimens etched in 1 M HCl at 30 °C under a static potential condition of (1) -0.4 V, (2) -0.45 V, (3) -0.5 V, (4) -0.55 V, (5) -0.6 V, (6) -0.7 V. (b) Magnification of current transients during the first 150 ms etching in (a).

Fig. 1b indicates that the current rises after the induction period and the slope increases significantly with the etch potential. When the etch potential is below -0.55 V, the current grows

continuously to the end of the experiment in this work. However, when the potential is above -0.55 V, the current rises to a maximum and then almost remains until the etching ends, forming a plateau in the curve. The current value of the plateau increase from 370 mA to 470 mA as the etch potential increases from -0.5 V to -0.4 V. Moreover, the appearing time of the plateau also becomes earlier as the etch potential increases. Appearing of the plateau in the current-time curve indicates that there is a limiting value for the current in the pitting behavior on Al in this work, and the limiting value is relevant to the etch potential. As the current-time reaches the plateau, the controlling factor of the pitting behavior changes from the etch potential to the etch current or maybe the current density.

3.2 Pit morphology during potentiostatic etching

Fig. 2 shows the current-time curves of the etching experiments with different times under the same potential condition and Fig. 3 shows the characteristic morphology of Al surface after the corresponding experiments. The curves in Fig. 2 exhibit a good reproducibility of the experiments in this work, and indicate that the current plateau appears at a time point between 550 ms to 600 ms. The pits morphologies on Al surface in Fig. 3 are apparent, showing clear edges, and the pits can be easily counted and measured. As the time of etching increases from 100 ms to 500 ms (Fig. 3a to Fig. 3e), it is found that the pit size grows gradually and the outlines of the pit-mouth are almost circular. A few pits with irregular shape may be found, but those are likely formed as several pits connect. Three dimensional structures of pits on the specimen, which is etched for 500 ms, are examined with AFM and the results are shown in Fig. 4. It is found in Fig. 4 that pits are all in the same shape of hemisphere although they are very different in size. On the other hand, the hemispherical shape also agrees well with the circular outlines of the pit-mouth exhibited in Fig. 3. These results indicate that the pits remain hemispherical after their nucleation and grow continuously during the etching before 500 ms.

When the etch time extends to 700 ms, all pits in Fig. 3f are found to be in the shape of half-cube and no hemispherical pit is observed. The half-cubic pits are reported to be the crystallographic pits formed during galvanostatic etching and the half-cubic shape is consistent with the dissolution of $\{1\ 0\ 0\}$ planes [19, 23]. Therefore it means that all of the hemispherical pits have turned into the half-cubic pits by 700 ms during the etching experiment. The hemispherical pits are apparently resulted from an isotropic etching. Contrarily, the half-cubic pits are relevant to the selective dissolution along the particular crystallographic direction. Therefore the pitting behavior on Al during the etching experiment has changed from isotropic to anisotropic by 700 ms, and the deformation of the hemispherical pits is resulted from the anisotropic etching which develops in the pits.

Fig. 2 indicates that the current plateau appears at a time point between 550 ms to 600 ms in the current-time curve. It agrees well with the time point shown in Fig. 3 when the hemispherical pits turn into half-cubic pits. Consequently, it indicates that during the etching, the pitting behavior remains isotropic and hemispherical pits develop at the current-rising stage. When current reaches the limiting value and the plateau appears, the pitting behavior changes to be anisotropic and the hemispherical pits quickly turn into the crystallographic pits of the half-cubic shape.

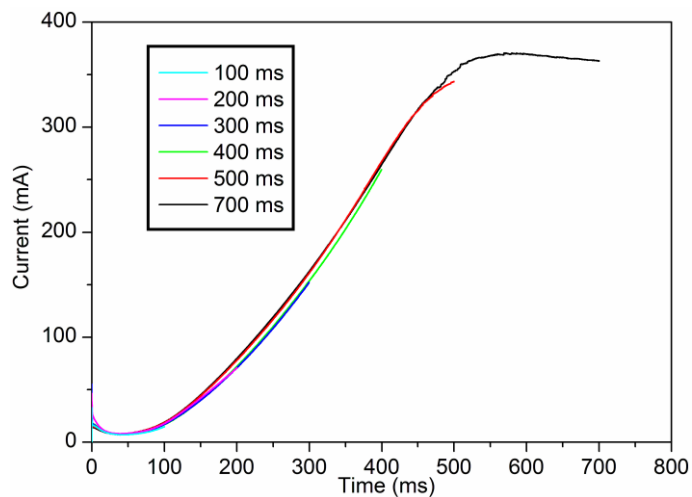


Figure 2. Current-time curves of Al specimens etched under the potential condition of -0.5 V for different times in 1 M HCl at 30 °C.

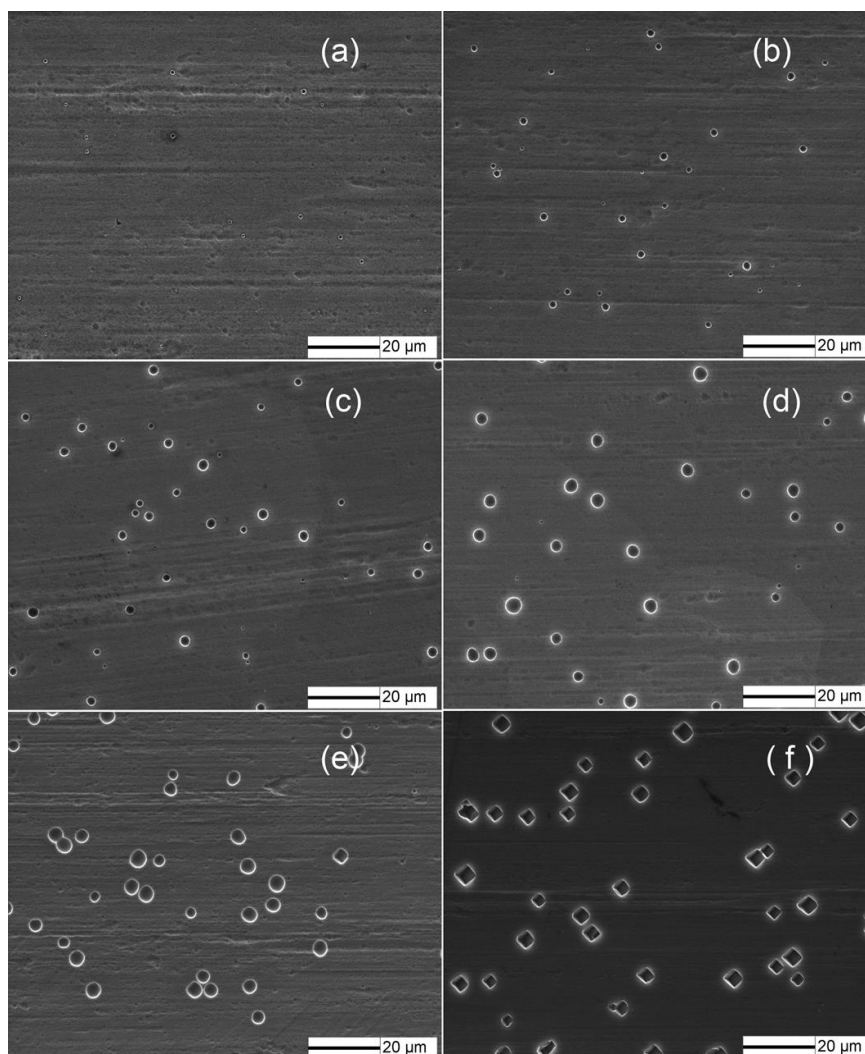


Figure 3. SEM image of Al surface etched under the potential condition of -0.5 V in 1 M HCl at 30 °C for (a) 100 ms, (b) 200ms, (c) 300 ms, (d) 400 ms and (e) 500 ms.

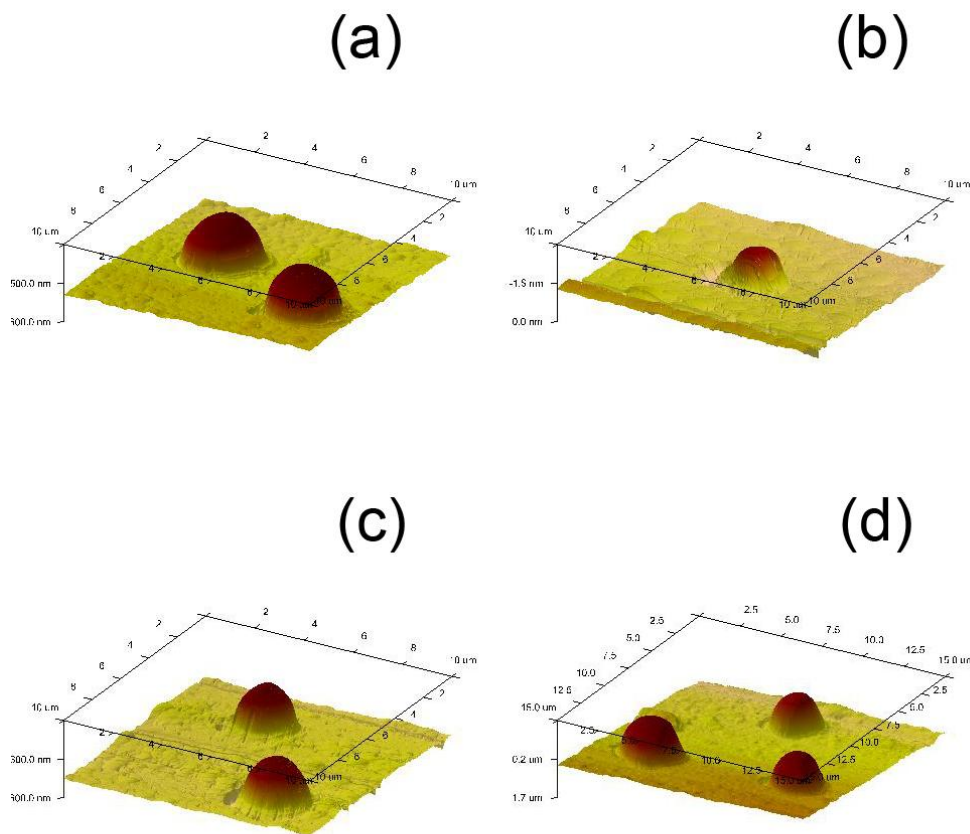


Figure 4. 3D images of pits in different sizes on Al specimen etched under the potential condition of -0.5 V in 1 M HCl at 30 °C for 500 ms.

3.3 Pit density and pit size distribution during potentiostatic etching

Fig. 5 shows the variation of pit number densities with time during the etching experiments under the potential condition of -0.5 V. Fig. 6 shows the diameter distribution of the hemispherical pits developed on specimen surface after the corresponding experiments in Fig. 2. The abscissas are labeled with the midpoints of each pit diameter class. The diameter distribution of pits after the experiment of 700 ms is not considered because the shape of pits has changed at that time.

Fig. 5 indicates that the pit density increases sharply before 300 ms, which reveals that the pit nucleation happens a lot. Fig. 6 shows that small pits $\leq 1 \mu\text{m}$, which are newly generated, always account for a large proportion before 300 ms. Between 300 ms and 500 ms, the pit density reduces slightly. However, it is hard to say that the pit nucleation ceases during the interval since it is found in Fig. 6d that small pits are still developed. The pit density decreases probably because plenty of small pits merge into the large ones while they keep on growing [19]. The histograms of pit diameter distribution in Fig. 6 shift toward the increasing of etch time before 500ms. It indicates that the early pits grow continuously into larger size while new pits arise. This means that the hemispherical pits remain active and keep on growing after their initiation. Growth of the hemispherical pit has ever been

reported [20]. The pit density changes little after 500 ms in Fig. 5. It is also found in Fig. 6e that only few pits $\leq 1 \mu\text{m}$ are observed at 500 ms. These results demonstrate that no new pit appears after then.

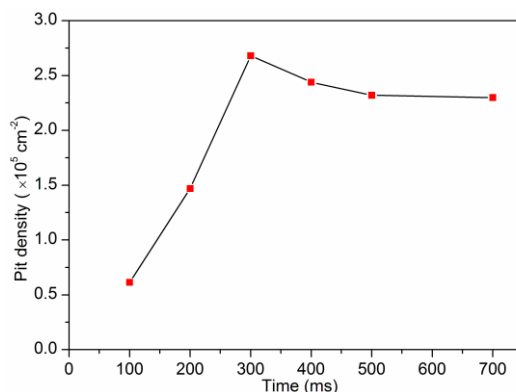


Figure 5. Variation of pit number density with time during the etching under the potential condition of -0.5 V in 1 M HCl at 30 °C.

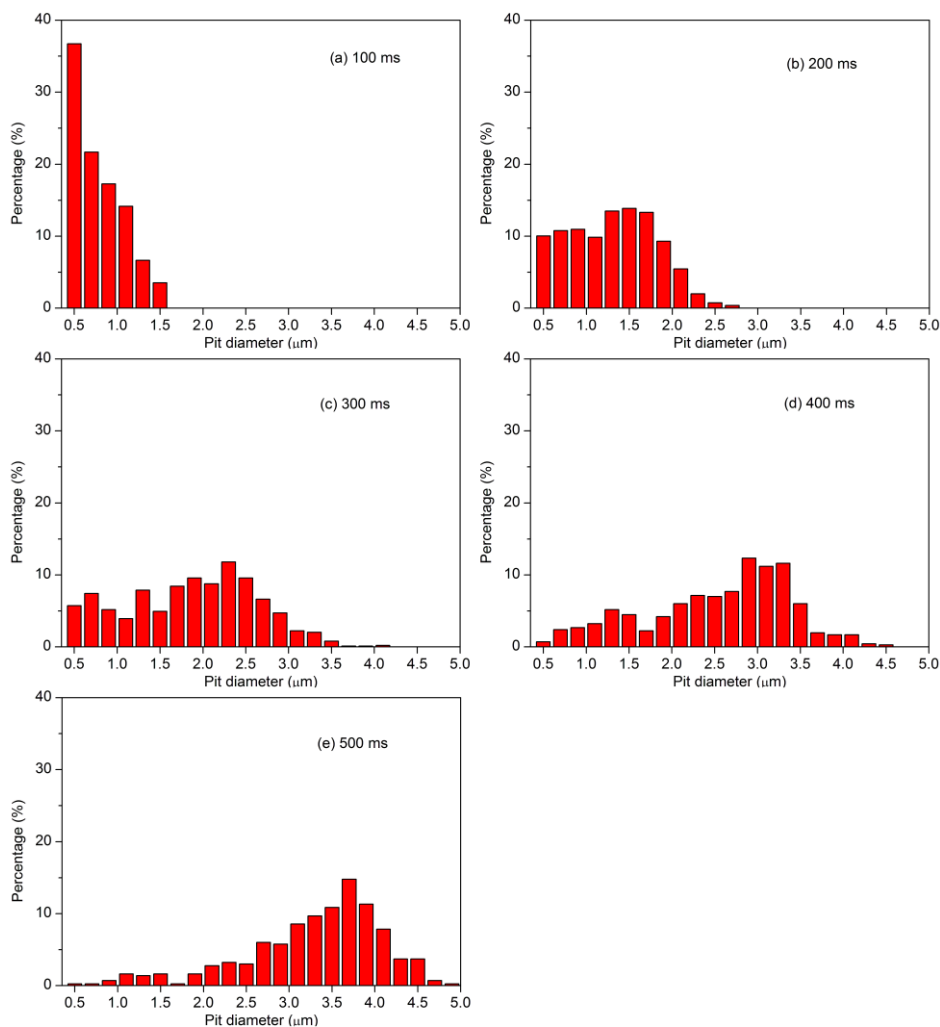


Figure 6. Pit diameter distribution on Al specimen etched under the potential condition of -0.5 V in 1 M HCl at 30 °C for (a) 100 ms, (b) 200ms, (c) 300 ms, (d) 400 ms and (e) 500 ms.

3.4 Current density for pitting during potentiostatic etching

It is known from above discussion that the hemispherical pits remain active and keep on growing after their initiation during the etching. Consequently, the current density for pitting during the etching can be calculated from the total area of all pits and the value of current in current-time curve. The total area of all pits, S_{pit} , is calculated from the pit density and pit diameter distribution according to:

$$S_{\text{pit}} = 0.5 \pi (d^2)_m \rho A \quad (1)$$

, in which $(d^2)_m$ is the mean of the square value of pit diameter, ρ is the pit density and A is the apparent area of specimen for the etching experiment.

The current density for pitting, i , is then calculated according to:

$$i = I / S_{\text{pit}} \quad (2)$$

, in which I is the value of current in current-time curve.

For the etching experiments in this work, A is 1 cm^2 , the values of $(d^2)_m$ are calculated from the statistical analysis of the as-obtained pit diameter distribution in Fig. 6, and the values of ρ have already been measured in Fig. 5. The value of I can be determined from current at the corresponding time point in Fig. 2. The result of the current density for pitting and its variation with time is exhibited in Fig. 7. It indicates that the current density for pitting continues reducing although the current in Fig. 2 increases before 500 ms. Therefore the current plateau appears when the current density for pitting reduces to a minimum. It implies that the change of the pitting behavior during the potentiostatic etching is controlled by the current density for pitting. As the current density decreases, it can not afford the dissolution of all planes in Al metal except for that in a particular crystallographic direction [27]. Then the pitting behavior changes from isotropic to anisotropic, resulting in that the hemispherical pits quickly transform into the crystallographic pits of the half-cubic shape.

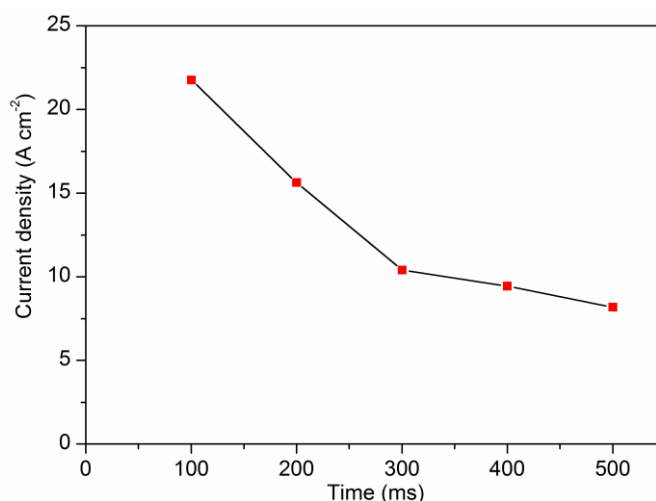


Figure 7. Variation of the pitting current density with time during the etching under the potential condition of -0.5 V in 1 M HCl at $30 \text{ }^\circ\text{C}$.

4. CONCLUSIONS

Potentiostatic etching during brief interval was conducted on Al foil specimen. The growth behavior of pits was examined with current transient measurement, SEM and AFM observation. The duration before the current reaches the minimum is the induction period of the pit nucleation and the period reduces significantly as the etch potential becomes more noble. The current rises to a maximum and a plateau appears during the etching. Hemispherical pits form and continue growing in size as the current rises before the plateau. When the current reaches the plateau, the pits quickly transform into the crystallographic pits of the half-cubic shape. The change of the pitting behavior is controlled by the current density for pitting. As the current density decreases, the pitting behavior changes from isotropic to anisotropic during the etching.

Reference

1. K. Nishio, K. Yasui, F. Matsumoto, K. Kanezawa, H. Masuda, *Adv. Mater.* 17 (2005) 1293-1295
2. H. Abd, Y. Al-Douri, N. Ahmed, U. Hashim, *Int. J. Electrochem. Sci.*, 8 (2013) 11461-11473
3. M. Amirhoseiny, Z. Hassan, S. S. Ng, *Int. J. Electrochem. Sci.*, 8 (2013) 5042-5051
4. J. Dian, M. Konecny, G. Broncova, M. Kronak, I. Matolinova, *Int. J. Electrochem. Sci.*, 8 (2013) 1559-1572
5. S. Langa, I. M. Tiginyanu, J. Carstensen, M. Christophersen, H. Foll, *Appl. Phys. Lett.* 82 (2003) 278-280
6. T. Fukushima, K. Nishio, H. Masuda, *Electrochem. Solid-State Lett.* 13 (2010) C9-C11
7. T. Fukushima, A. Takeda, K. Nishio, H. Masuda, *Electrochem. Solid-State Lett.* 13 (2010) C17-C19
8. B. W. Davis, P. J. Moran, P. M. Natishan, *Corros. Sci.* 42 (2000) 2187-2192
9. J. H. Seo, J. H. Ryu, D. N. Lee, *J. Electrochem. Soc.* 150 (2003) B433-B438
10. C. K. Dyer, R. S. Alwitt, *J. Electrochem. Soc.* 128 (1981) 300-305
11. R. S. Alwitt, H. Uchi, T. R. Beck, R. C. Alkire, *J. Electrochem. Soc.* 131 (1984) 13-17
12. D. Goad, *J. Electrochem. Soc.* 144 (1997) 1965-1971
13. T. Makino, R. S. Alwitt, S. Ono, *J. Electrochem. Soc.* 154 (2007) C132-C137
14. R. Xiao, K. Yan, *Corros. Sci.* 50 (2008) 3256-3260
15. L. Liang, Y. He, H. Song, X. Yang, X. Cai, C. Xiong, Y. Li, *Corros. Sci.* 70 (2013) 180-187
16. H. Park, C. Lee, H. Cho, T. Kim, S. Suh, *Surf. Interface Anal.* 44 (2012) 1423-1426
17. Z. Hou, J. Zeng, J. Chen, S. Liao, *Mater. Chem. Phys.* 123 (2010) 625-628
18. S. Ono, H. Habazaki, *Corros. Sci.* 51 (2009) 2364-2370
19. N. Osawa, K. Fukuoka, *Corros. Sci.* 42 (2000) 585-594
20. S. Ono, H. Habazaki, *Corros. Sci.* 53 (2011) 3521-3525
21. S. Ono, H. Habazaki, *Corros. Sci.* 52 (2010) 2164-2171
22. L. Yao, J. Liu, S. Li, M. Yu, *Corros. Sci.* 80 (2014) 12-18
23. S. Ono, T. Makino, R. S. Alwitt, *J. Electrochem. Soc.* 152 (2005) B39-B44
24. B. J. Wiersma, K. R. Hebert, *J. Electrochem. Soc.* 138 (1991) 48-54
25. C. F. Lin, K. R. Hebert, *J. Electrochem. Soc.* 137 (1990) 3723-3730
26. J. Lee, J. Kim, J. Kim, J. Lee, H. Chung, Y. Tak, *Corros. Sci.* 51 (2009) 1501-1505
27. J. H. Jeong, C. H. Choi, D. N. Lee, *J. Mater. Sci.* 31 (1996) 5811-5815